6
SOLID EARTH MODELLING PROGRAMME

Solid Earth Modelling group research activities are multidisciplinary (Engineering and Earth Sciences) and multi-component (GNSS Geodesy, computational seismology, geology, geophysics, physics and modelling). The major focus of the group is data analysis and modelling to gain significant insights in to sub-surface process in the earth's crust. During the year 2013-2014 group has contributed to GNSS based deformation modelling along the 2500 Km Himalayan arc from Ladakh Himalaya in the west to Arunachal Himalaya in the east, Slip models for 2004 Sumatra-Andaman rupture, establishment of real-time data telemetry VSAT's for Andaman GNSS Network, GPS measurements for landslide deformation monitoring, GPS observations south of Palghat-Cavery shear zone to study the zonal variability of tectonic co-seismic deformation, seasonal perturbations in Inter-seismic deformation of North-East India. In the field of tectonic-geomorphology, research focus was on Nahan Salient of Western Indian Sub-Himalaya and drivers of drainage growth in an actively uplifting area. In computational seismology the group had majorly contributed to seismic hazard studies in Indian subcontinent as a whole as well as specific seismic hazard assessment in Himalayas, Gujarat and peninsular India. During this year, we have initiated seismic broad band experiment in Kashmir Himalayas, studied crustal structure of Dharwar region along E-W corridor and estimated the source process of the Sikkim earthquake (18th September 2011), In addition we have used finite element method to gain significant insights in to wave propagation and deformation in different medium.

Inside

- *Contemporary Deformation in the Kashmir-Himachal, Garhwal and Kumaon Himalaya: Significant insights from 1995-2008 GPS time series*
- *Seasonal perturbations in inter-seismic deformation of North-East India*
- *GPS Geodetic Observations in Southern Peninsular India to study the pre, co & post seismic deformations associated with 2012 M8.6 Indian ocean strike slip earthquakes*
- *Establishment of Continuous mode GPS station and landslide observation using GPS Geodetic Observations*
- *Absence of Intermontane valleys in the Nahan Salient of Western Indian Sub-Himalaya*
- *Active uplift, surface relief and mass redistribution drive drainage growth*
- *Seismic hazard and risks estimates for Himalayas and surrounding regions based on the Unified Scaling Law for Earthquakes*
- *The role of microzonation in estimating earthquake risk*
- *Probabilistic seismic hazard assessment for Gujarat region of western India: An Application of a Bayesian extreme-value model of the Results*
- *Estimation of Peak Ground Acceleration (PGA) in Peninsular India for Hazard Analysis.*
- *Neo-Deterministic Seismic Hazard Map of India*
- *Crustal imaging of Dharwar Region across E-W Corridor*
- *Seismic Broadband Experiment in Kashmir Himalayas*
- *Finite Element Method for Deformation in Porous Thermoelastic Material with Temperature Dependent Properties*
- *Finite Element Analysis of Wave Propagation in Thermoelastic Saturated Porous Medium*
- *Finite Element Method for Transient Wave Problem in Thermoelastic Saturated Poro-Viscoelastic Medium*
- *2004 M 9.3 Sumatra-Andaman Rupture Extent and Slip Distribution, and its Implications on the Regional Tectonics.*
- *Establishment of Real-Time Data Telemetry VSAT's for Andaman GNSS Network.*
- *Source Process of the Sikkim Earthquake 18th September, 2011, Inferred from Tele-seismic Body-wave Inversion.*

6.1 Inverse Modelling of GPS-derived Present Day Active Deformation in Ladakh Himalaya by CSIR-4PI (erstwhile C-MMACS) Scientists

Inverse modeling GPS derived deformation rates over an eleven year period indicate low slip rate of Karakoram fault suggesting that the motion of Tibet does not confirm to plate-like motion which would result in rapid strike slip motion along the Karakoram fault. Instead, large-scale tectonics in Tibet is best described as deformation of a continuous medium where the slip rates on the strike slip faults differ little from those on normal and thrust faults, and all faults constitute passive markers of discontinuities in the strain field that translate and rotate with a deforming continuum.

Sridevi Jade

6.2 Global Navigation Satellite Systems (GNSS) and Earthquake Hazard

GNSS geodetic studies over two decades have given precise and accurate quantitative estimates on the persistent northeastward motion of the Indian plate with the plate-tectonic velocities varying from 5.94 cm/yr at Maldives in the south to 3.18 cm/yr at Leh, located in Ladakh Himalaya. This considerable reduction in velocity of ~3 cm/yr is largely being accommodated in the plate boundary zone where Indian plate thrusts beneath the Eurasian plate. This change in velocity i.e. baseline shortening between two sites causes high stress buildup and strain accumulation along the plate boundary regions which in intermittently released as earthquakes.

Sridevi Jade

6.3 Seismotectonic Implications of Strike–slip Earthquakes in the Darjiling–Sikkim Himalaya

The 18 September 2011 (*Mw* 6.9) strike–slip event suggests that the Darjiling Sikkim Himalaya (DSH) is likely to contain an active transverse strike–slip faulting. High-precision Global Positioning System measurements (1997–2006) indicate that a maximum of ~4 mm/year convergence is being accommodated in this region and DSH is locked south of 27ºN both east and west of GTF (Gish Transverse Fault) about 10 km north of the Himalayan mountain front. About 3–4 mm/year sinistral strike–slip is postulated on GTF north of 27ºN.

Dislocation based forward modelling using two thrust dislocations with oblique slip and a sinistral strike–slip dislocation generated velocities that were closest to the measured back-slip velocity field in DSH. Given all this, the role of transverse zones in Himalayan deformation may be significant and must be therefore studied and better understood. These observations suggest that a fresh look at our ideas on the Himalayan deformation is required as it appears to be more complex than visualized by the current models.

Malay Mukul, Sridevi Jade, Kutubuddin A, Matin A

6.4 Contemporary Deformation in the Kashmir-Himachal, Garhwal and Kumaon Himalaya: Significant Insights from 1995-2008 GPS time series

Time-averaged (1995-2008) GPS derived surface velocities, convergence and extension rates along arc-normal transects in Kumaon, Garhwal and Kashmir-Himachal regions in the Indian Himalaya indicate that this region is accommodating ~ 2 cm/yr of the India-Eurasia plate motion (~4 cm/yr). The total arc-normal shortening of the northwest Himalayan wedge varies between ~10 -14mm/yr which is being accommodated differentially along the arc-normal transects; ~5-10 mm/yr in Lesser Himalaya and 3-4 mm/yr in Higher Himalaya. Most of the convergence in the Lesser Himalaya of Garhwal and Kumaon is being accommodated just south of the MCT (Main Central Thrust) fault trace, indicating high strain accumulation in this region which is also consistent with the high seismic activity in this region. Also for the first time an arc-normal extension has also been observed in the Tethyan Himalaya of Kumaon. In addition the results also gave an estimate of co-seismic and post-seismic motion associated with the 1999 Chamoli earthquake which is modeled to derive the slip and geometry of the rupture plane.

Sridevi Jade, Malay Mukul, Gaur V K, Kumar K, Shrungeshwar T S, Satyal G S, Dumka R K, Jagannathan S, Ananda M B, Dileep Kumar P, Banerjee S

6.5 Seasonal Perturbations in Inter-seismic Deformation of North-East India

GPS time series is a manifestation of long term plate motion along with contribution from some non-tectonic forcing. The non-tectonic forces causing deformation of the crust are, to say a few, ocean and body tides of the Earth, interhemispheirc exchange of fluids, snow melt, groundwater runoff, Glacial Isostatic adjustment, atmospheric loading, etc. The Earth as a whole responds to external forces as an elastic body. As was shown by Darwin in 1882, changes of the weight of the atmospheric column due to variations of pressure result in “distortion of the upper strata of the Earth” [i.e. deformation of the crust] called atmospheric pressure loading [http://gemini.gsfc.nasa.gov/aplo/]. The magnitude of the effect can be up to 15-20mm and it can

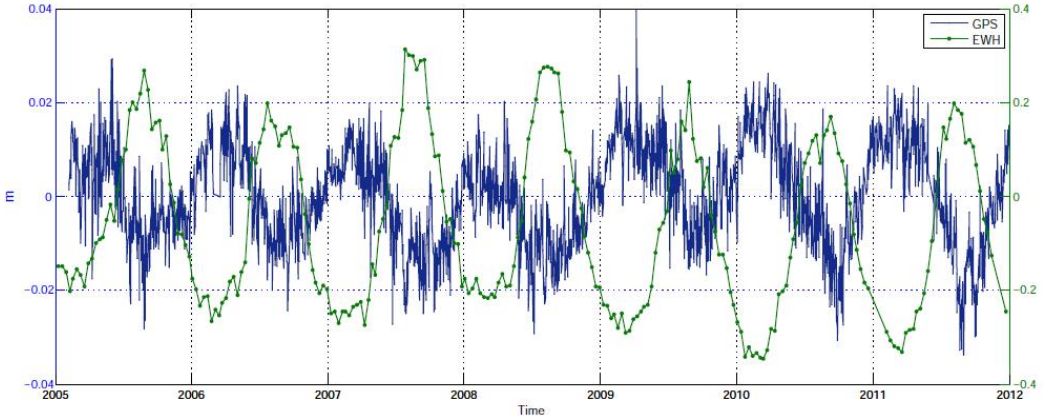

Figure 6.1 Comparison of GPS vertical time series of Tezpur and GRACE derived equivalent water thickness

vary as much as 10mm within a 24 hour period. As a result, this physical phenomenon affects the coordinates of geodetic sites (VLBI, GPS, SLR, DORIS etc) and should be accounted for in all high precision geodetic analyses. On the other hand, the solid Earth crust also deforms due to the largest mass movement on the solid earth through global hydrological cycle, the exchange of water between ocean, land, and ice sheets. We have studied the hydrological loading and its effect on crust in North Eastern India using GPS and GRACE (figure 6.1). The deformation reaches up to ~10-20mm in vertical whereas ~2-3mm in horizontal components. In addition, power spectral analysis of GPS time series is opted to find out the frequency of perturbations and seasonality in the time series. Power spectral densities demonstrate that colored noise is mostly abundant in the lower frequency domains whereas at higher frequencies the spectrum mostly corresponds to white noise (figure 6.2). The spectral index of most components are within -1<α<1 and suggest a dominance of fractal white noise in the time series. Autocorrelation studies also favoring the presence of white noise by showing highest peak at iΔt=0. In order to investigate the seasonality, time series is decomposed to find its trend and the seasonal signal has been extracted from the power spectrum. The power spectrum of every component (North, East and Up) shows its biggest peak at 0.73cycles/year and next prominent peak is found at 2.15cycles/year at one of the stations. This assessment of deformation associated with non-tectonic forcing, like atmospheric loading, along with tectonics is vital since it not only affects the earthquake nucleation process and stress build up in the crust but also effectively alters the drainage pattern which is the lifeline of the North-Eastern India.

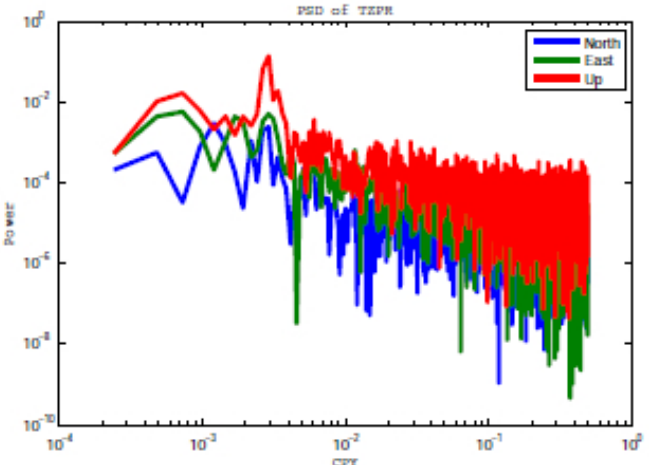

Figure 6.2 Power spectra of Tezpur GPS time series

Jagat Dwipendra Ray[1], Vijayan M S M and Ashok Kumar[1]
[1]Tezpur University, Tezpur

6.6 GPS Geodetic Observations in Southern Peninsular India to study the Pre, Co & Post Seismic Deformations Associated with 2012 M8.6 Indian Ocean Strike Slip Earthquakes

On 11th April 2012 a strike-slip earthquake of magnitude M8.6 – 13th strongest earthquake since 1900 as well as strongest strike slip earthquake ever recorded in human history – struck the Indian ocean basin west of Sumatra-Andaman subduction zone with an unprecedented after shock of magnitude M8.2 within two hours. The earthquake occurred at Indo-Australian diffused tectonic boundary and it was felt in Indian, Australian as well as Sunda plates. From the magnitude, nature and location it was attributed to a rare event associated with major plate boundary process of tectonic scale which may happen once in million years. A GPS geodetic

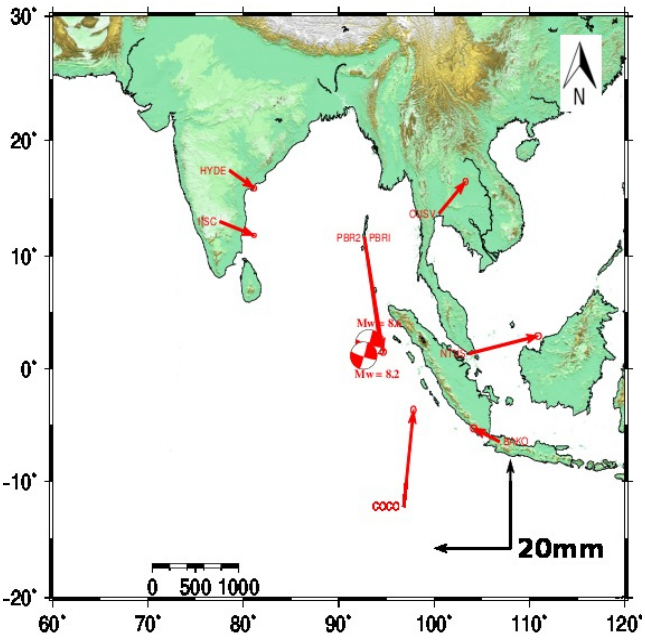

Figure 6.3 Map Showing the co-seismic displacement at IGS stations associated with 11th April 2012 Indian Ocean strike slip earthquakes

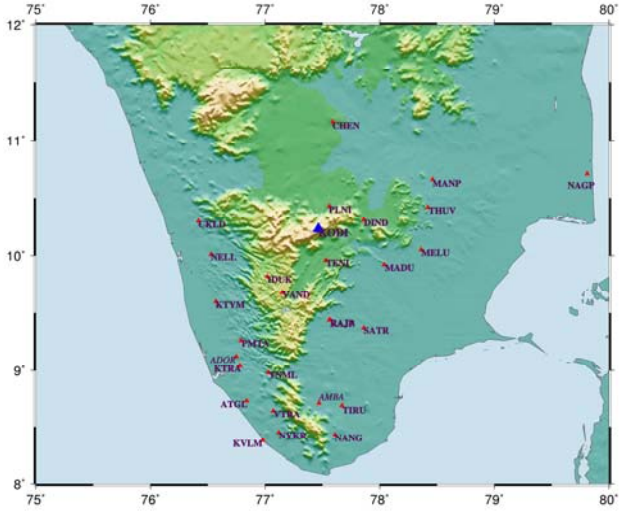

Figure 6.4 Map showing the campaign stations of southern peninsular India where GPS geodetic observations were carried out.

investigation was carried out using IGS station observations to study the impact of such a strongest and rare earthquake on the deformation of the crust.

Co-seismic deformation associated with the strongest earthquakes were estimated using the observations from IGS stations situated in Australian plate, Indian plate, African plate, Philipine plate and Andaman micro plate. The results of this preliminary study show the large scale deformation at sites situated in different tectonic plates as far as thousands of kilometers away from the epicenter (figure 6.3). Indian sites in peninsular India has displaced from 7.7 to 9.6 mm towards SSE direction. In order to further refine the co and post-seismic deformation pattern across the faults, lineaments and shear zones of Southern peninsular India associated with such strongest earthquakes, GPS based geodetic observation campaign was carried out from September to October 2013.

The GPS based geodetic observations were carried out at 31 stations south of Palghat-Cavery shear zone for the period of 3 continuous days at each station (figure 6.4). The observations will be useful to study the zonal variability of tectonic co-seismic deformation in this region in addition to the deformation across the Achan-Kovil shear zone.

Vijayan M S M, Simon Justin, Shrungesh T S and Anil Earnest

6.7 Establishment of Continuous Mode GPS station and Landslide Observation using GPS Geodetic Observations

A new study has taken up as part of the 12th FYP EDMISSIBLE to study the landslides using GPS based observations in collaboration with CSIR CBRI, Roorkee. Two landslides has been

Figure 6.5 GPS observation points in the two selected landslides in Chamoli districts of Uttarakhand

Figure 6.6 Continuous mode GPS geodetic observation facility at CSIR CBRI, Roorkee established by CSIR-4PI (ERSTWHILE C-MMACS). Insert shows (left) the web interface and (right) the instrument setup.

identified by CSIR CBRI in Chamoli district of Uttarakhand (Figure 6.5). *CSIR-4PI* (erstwhile C-MMACS*)* and CSIR CBRI has carried out first GPS based geodetic survey at various points on the landslides to study the stability. Prior to the campaign mode observation, a continuous mode GPS geodetic observation facility has been established at CSIR CBRI, Roorke and a real-time data stream has been established with CSIR-4PI (erstwhile C-MMACS) and CSIR CBRI for continuous monitoring (Figure 6.6). These observations will be used along with consecutive campaigns in the forthcoming years to study the landslides.

Vijayan M S M, Shrungesh T S, Sarkar S, Kanungo D P*, Amit Rana1 and AnilMaleta**
*CSIR CBRI, Roorkee

6.8 Absence of Intermontane Valleys in the Nahan Salient of Western Indian Sub-Himalaya

Direct evidence of faulting along the Himalayan mountain front is very rare. The most conspicuous indicators for the presence of a structural discontinuity and an active tectonic boundary are manifested in the geomorphology. In most of the cases, a topographic break defines the outermost Himalayan thrust fault i.e. Himalayan Frontal Thrust (HFT). However, the

nature of this tectono-geomorohic boundary tends to vary significantly along the strike of the mountain belt. In some sectors, it is marked by the presence of elongated intermontane valleys popularly known as 'duns', whereas other sectors are conspicuous by their absence. The Nahan sector of the Western Indian Himalaya is one such area that is characterized by the absence of intermontane valley. Here, in this article we emphasize that the absence of intermontane valleys in the Nahan sector gives rise to a distinctive geomorphic expression of the active tectonic boundary. In the Nahan sector, active slip along the underlying thrust faults and splays has resulted in the accumulation of high relief spread over a relatively smaller area. This led to the absence of the duns in this area. Also, the topographic boundary closely corresponds to a number of drainage anomalies establishing the active tectonic nature of the HFT. The drainage anomalies mainly include the deflection of streams, widening of channels and increase in their sinuosity as they approach the mountain front. The increase in the sinuosity of the channels is also marked by degradation activity and presence of broad flat terrace surface that confirm to the tectonic uplift in this area.

Figure 6.7 Field manifestation of the Himalayan Frontal Thrust (HFT) in the Nahan Salient.

Singh T, Awasthi A K[1], Ravindra Kumar[2] and Virdi N S[3]
[1]Graphic Era University, Dehradun, [2]Panjab University, Chandigarh.
[3]Wadia Institute of Himalayan Geology, Dehradun.

6.9 Active Uplift, Surface Relief and Mass Redistribution Drive Drainage Growth

As the topography builds up, surface relief tends to increase and interact with the surface processes, mainly drainage system. Evolution and growth of drainage are part of the whole process. Drainage basins spread over different spatial scales have been used to gauge subtle uplifts along small active faults traces and also along large spreading fault-related folds (ridges) etc. We look into the drivers of drainage growth in an actively uplifting area. At the same time we investigate the mode by which drainage basins grow over time. In the same context, we investigate the growth of drainage basins and its relationship with the surface relief.

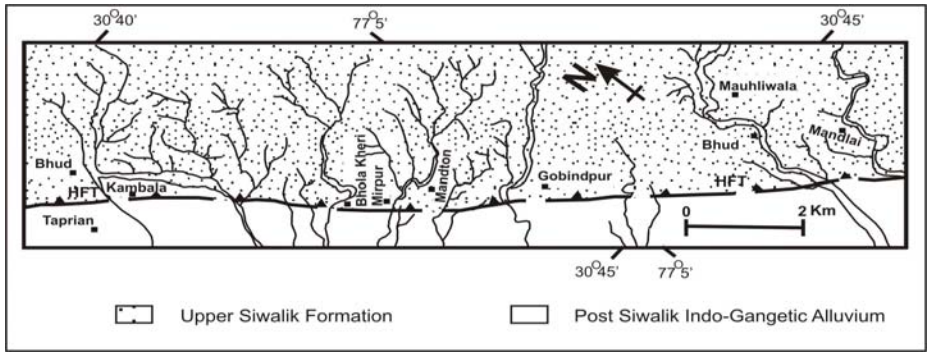

Figure 6.8 Coalescence and lateral migration of drainage as alternate ways of network evolution.

Our investigations reveal that the drainage basins evolve by maintaining their elongation ratios. Local increase in surface slope induces the drainage basins to look for alternative modes of evolution i.e. coalescence, lateral migration and headward growth etc. In conclusion, both different growth modes together play a dominant role in redistribution of mass from actively uplifting areas to adjoin depocentres through drainage basin growth.

Tejpal Singh, Awasthi A K[1], Janani Srinivasan[2], Kanmani Kamaraj[2], Rebba Mary Raju[2], Sreeraj T[2], [1]Graphic Era University Dehradun, [2]Bharathidasan University, Tiruchirappalli

6.10 Seismic Hazard and Risks Estimates for Himalayas and Surrounding Regions Based on the Unified Scaling Law for Earthquakes

This paper has been completed under the Indo-Russian DST-RFBR project sponsored by Department of Science and Technology, Government of India and Russian Foundation for Basic Research, Russian Federation. In this paper, we accept the hypothesis that the seismic process is self-similar, at least locally, and estimates the coefficients A, B, and C using the Scaling Coefficients Estimation (SCE) algorithm. We analyze the earthquake catalog from USGS/NEIC and provide the maps of the A, B, and C coefficients for the different scales and discuss their likely relationship with the observed continental deformation and related structure of the Earth. The parameters A, B, and C of this Unified Scaling Law for Earthquakes (USLE) in Himalayas and surrounding regions have been studied on the basis of a variable space and time scale approach. The observed temporal variability of the A, B, and C coefficients indicates significant changes of seismic activity at the time scales of a few decades. For Himalayan region, the values of A, B and C have been estimated mainly ranging from -1.6 to -1.0, from 0.8 to 1.3, and from 1.0 to 1.4, respectively. Figure 1 demonstrates the distribution of the estimated values for each of the three USLE coefficients and using these coefficients the expected maximum magnitude M with 1% and 10% probability of exceedance in 50 years based of the higher resolution settings and rich seismic data have been estimated.

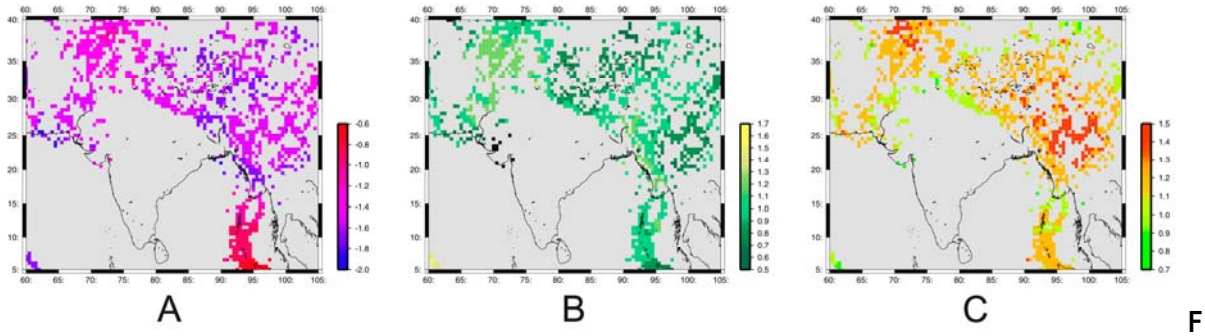

F

Figure 6.9 The distribution of the USLE coefficients in space (based on the USGS/NEIC Global Hypocenters Database Systems, 1965-2011).

For more comprehensive estimation of seismic hazard, we complement the final map of the expected maximum magnitude M based on USLE with the reported maximum magnitude in 1900-2010 to estimate the hazard map of expected ground shaking in terms of PGA. In order to

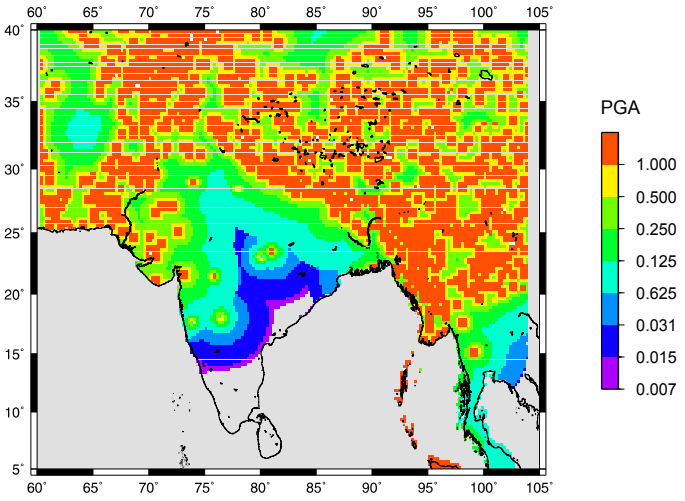

Figure 6.10 Final deterministic seismic hazard map

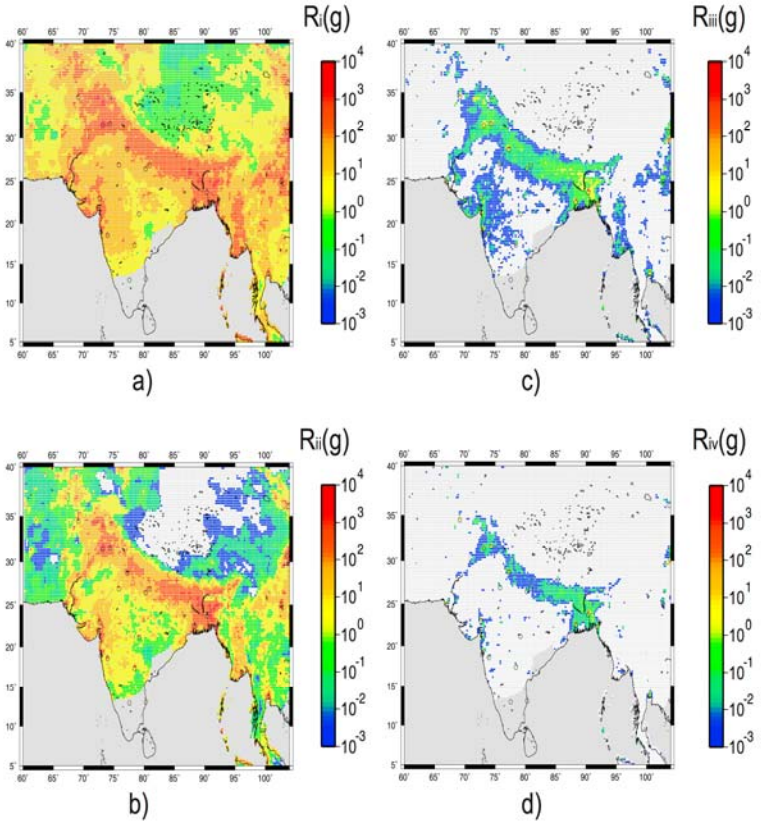

Figure 6.11 Oversimplified convolutions of seismic hazard map H(g) with the population density distribution

produce deterministic seismic hazard map, a source-receiver distance is the estimated at a grid of 0.25° x 0.25° and for each source of different magnitude, PGA is calculated and the maximum at each cell is plotted as shown in Figure 6.10.

Any kind of risk estimates results from a convolution of the hazard with the exposed object under consideration along with its vulnerability –

$$R(g)=H(g) \star O(g) \star V(O(g)),$$

Where H(g) is natural hazard at location g, O(g) is the exposure of objects at risk at g, and V(O) is the vulnerability of objects at risk.

Using the population density distribution based on Gridded Population of the World, Version3 (GPWv3 for 2010, we estimated the seismic risks in four levels (figure 6.11), each of the four risk scales is covering the top seven decimal orders of the risk values, so that the cells in red are 1000000 times more dangerous than those in blue. The collapse of the risky areas to the region of the densest population appears rather natural demonstrating how non-linearity of conditions changes expectation of seismic risk. It is notable that, as expected, the mega-cities and their agglomerations are at the top of risk distributions.

Imtiyaz A Parvez, Anastasia Nekrasova and Vladimir Kossobokov**
*Institute of Earthquake Prediction Theory & Mathematical Geophysics, Moscow

6.11 The Role of Microzonation in Estimating Earthquake Risk

This work is dedicated to understand the role of seismic zonation and microzonation, as well as understanding seismic risk analysis and mitigation strategy. The merits and demerits of various approaches to estimating earthquake hazard are discussed in terms of whether it is probabilistic, deterministic, or neodeterministic. The importance of geotechnical, geomorphological, and geological databases for seismic microzonation has been highlighted along with various techniques available to characterize site conditions. A variety of tools currently in use illustrate the basic principles of microzonation mapping at different scales. The main parameters involved in earthquake loss assessments and evaluating the influence of soil conditions on these estimates are discussed using Earthquake Loss Assessment for Response and Mitigation (QLARM), an advanced seismic risk estimation tool, for a few case histories. Various numerical and experimental methods express the local soil response to ground shaking. Discussions among scientists on the best parameter or parameters to define site conditions are not closed. Vs values that tend to be commonly used in national building codes and recent Ground Motion Prediction Equation (GPMEs) are one of them, but recent studies indicate that it could misestimate site amplification. We presented a few other parameters that help in defining the site effect. For example, the advanced study aimed at Neodeterministic Seismic Hazard Assessment (NDSHA) allow for the development of a set of regional and local scale maps of the expected ground motion at bedrock and surface level, based on the physical modeling of ground shaking from a wide set of possible scenario earthquakes. These maps can be defined in terms of peak ground displacement, velocity, acceleration, or any other ground motion parameter that can be extracted from the set of complete synthetic seismograms describing ground shaking at the different sites. Recently, displacement-based and energy approaches have made significant advances. The former approach is based on the assumption that limiting displacement demands can reduce structural and nonstructural damage; the displacement response spectrum, as the input, is of great significance to displacement based design just as the acceleration response spectrum is to the traditional force based design. The latter approach, beyond the potentiality of designing earthquake-resistant structures by balancing energy demands and supplies, allows us to properly characterize the different types of time histories (impulsive, periodic, with long duration pulses, etc.) that may correspond to an earthquake ground shaking, simultaneously considering the dynamic response of a structure. Earthquake risk assessment requires various types of data that are often disconnected from microzonation ones because their implementation remains tricky. Indeed, it is not straightforward to use existing microzonation data in seismic scenarios because relationships to derive amplification factor from parameters used to define site conditions are missing. Research in this direction should improve the estimate in the future.

Imtiyaz A Parvez and Philippe Rosset*
*WAPMERR, Geneva, Switzerland

6.12 Probabilistic Seismic Hazard Assessment for Gujarat Region of Western India: An Application of a Bayesian Extreme-Value Model of the Results

Amongst all hazard assessment techniques available presently, Bayesian theory provides a more reliable measure of hazard assessment and it has the unique feature that we can add new data on availability to obtain a realistic evaluation of seismic hazard. Here, the approach of Bayesian extreme-value distribution is adopted to evaluate hazard parameters for Gujarat region. The seismic moment, slip rate, earthquake recurrence rate and magnitude frequency parameters are the basic parameters to obtain the prior estimate of seismicity. We prepared the earthquake data set of magnitude Mw ≥ 4.0, spanning the period from 1330 to 2012 using a catalogue of national and International and other published catalogues to prepare a reliable, homogeneous and complete earthquake catalogue in terms of all magnitude types from 1705 to 2012 in view of completeness. The entire region is divided into three seismogenic zones (figure 6.12) on the basis of seismotectonics, historical and current seismicity, clustering of events and geological lineament. These are Kachchh, Saurashtra and Gujarat mainland zone. We computed the probability for T=2, 5, 10, 20, 50 and 100 years for each zone.

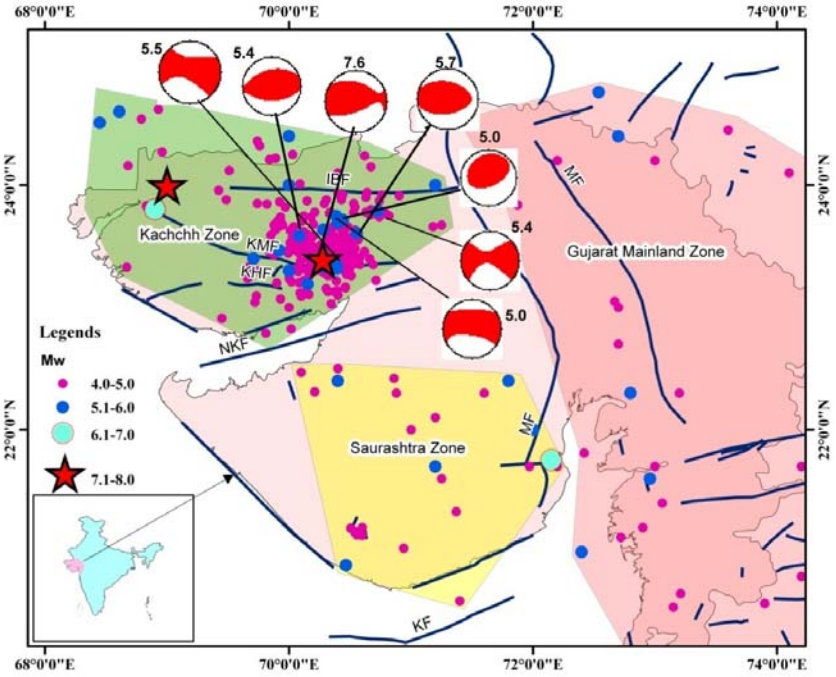

Figure 6.12 Seismotectonics features and epicentral location of earthquakes with three zones namely Kachchh, Saurashtra and Gujarat Mainland based on the local geology and earthquake clusters.

We adopted the well-known approach of extreme-value statistics and used Bayesian analysis imposing magnitude distribution using the Gutenberg-Richter b-value. The random variables α and β are estimated by means of Bayes' theorem with prior distributions. In the statistical methods, normally a large number of observations are needed to estimate return periods and probabilities. We have used seismicity data of 308 years to analyze the earthquake hazard parameters and probability of occurrence. Prior values of the parameters are estimated based

on the maximum likelihood criterion. The seismic hazard is described in the form of hazard curves i.e. probabilities versus magnitude for short-term and long-term period in each zone. For the Gujarat region, first time we obtained probability using Bayesian model.

The Kachchh region exhibits higher probability for occurrence of moderate to strong magnitude and Saurashtra and Gujarat mainland shows moderate probability for the same. The variation in probability for Saurashtra zone and Gujarat mainland zone is higher compared to Kachchh zone but the probability of occurrence of earthquakes is less in both these zones compared to Kachchh zone for the same coefficient of variances. These results have potentially useful implications in the probabilistic seismic hazard assessment for the entire Gujarat state. The zone wise comparative seismic hazard categorization could be useful for design purposes to identify the priority regions for earthquake resistant designs. The seismic potentiality presented in this study can be interpreted for both short-term as well as for long-term seismic hazard, especially, for region like Kachchh which witnessed several moderate to large earthquakes in the past and recent past and aftershock activity is still going on in the region after the Jan 26, 2001 Bhuj (M_w 7.7) earthquake. Consequently, this region is more vulnerable to moderate to large earthquakes in near future.

*Imtiyaz A Parvez and Parul C Trivedi**
*India Meteorological Department, Ahmedabad

6.13 Estimation of Peak Ground Acceleration (PGA) in Peninsular India for Hazard Analysis.

Peninsular India, normally considered as a stable continental part of the Indian subcontin ent, has experienced several damaging earthquakes of magnitude greater than 6.0 in last couple of decades. Earthquakes occurred in various places in Peninsular India: Latur (1993: Mw 6.1), Jabalpur (1997, Mw 5.8) and recent Bhuj (2001, mw 7.6), which has claimed thousands of precious lives and damage to infrastructure accounted for huge economic losses (Figure 6.13). Although occurrence of large earthquakes is very low of an order of several decade to centuries but impact on society is very high. Thus, it becomes important to quantify the Peninsula Hazard for future events in terms of possible ground shaking. A comprehensive earthquake database with location, date and magnitude of past earthquakes is required to estimate reliable seismic hazard parameters to be used in a hazard study. The Catalog used in this study has been generated based on available information from various sources. Most recent events included from International Seismologicl Centre (ISC) and Preliminary Determination of Earthquakes (PDE) data (National Earthquake Information Center [NEIC]). Generally instrumental and more reliable data is available after 1960 from ISC, from US Geological Surveys USGS since 1973 and India Meteorological Department (IMD). After collection of the earthquake data from various sources, pre and aftershocks had been removed from the catalog as earthquake assumes to be occurred independently. Regression analysis has been made on Harvard Centroid Moment Tensor (CMT) data to establish various magnitude conversion relations and all magnitude converted to Moment magnitude (Mw) for the peninsular Indian catalog.

The seismicity parameters, (*a, b*) from Gutenberg Richter formula, first estimated for complete peninsular catalog for two different period (1800-2011) and (1960-2011). In both cases *b* values are very low 0.68 and 0.79. Source zone 1, which represents Gujarat region, exhibits very low *b* values and represents a region close to transformation boundary. Therefore, the catalog dataset was divided into sets for Gujarat region and Peninsular India (Excluding Gujarat or source zone 1). A very low value estimated from Gujarat catalog while rest of the data from peninsular India (Excluding Gujarat) gave *b* value 1.08 which is in line with global value for a larger region.

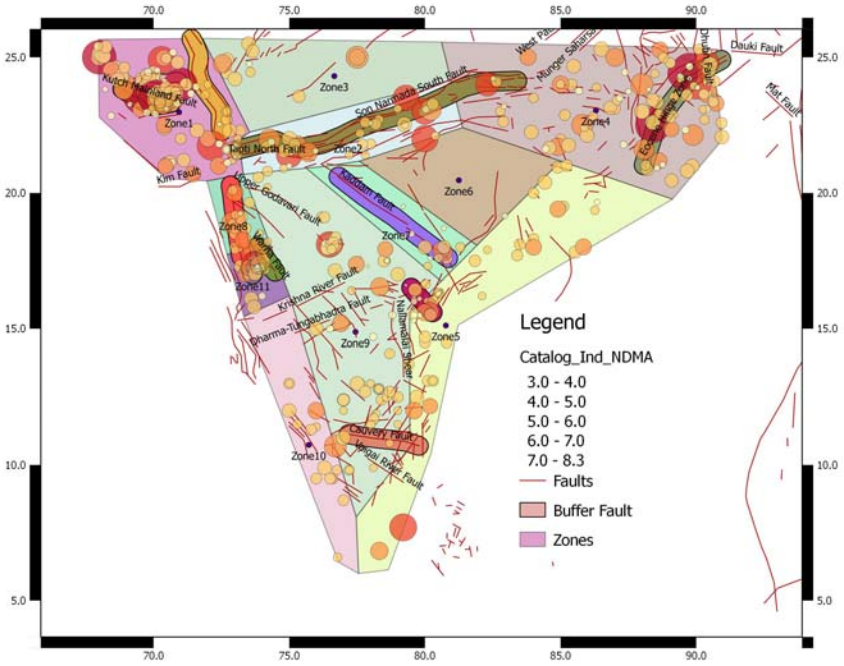

Figure 6.13 Map showing fault map (Seismotectonic Atlas of GSI) of Peninsular India with Earthquake catalog (circle). Color and size of circle indicate magnitude of the earthquake. Buffer zones are representing buffers generated for fault model.

Three data models have been generated for the computation of Hazard map: Classical Seismic Zones, Point Source and Fault Model. The Peninsular India region is divided into ten-source zones based on geology, earthquakes distribution and faults. Smaller zones do not have a sufficient number of earthquakes to perform credible statistical analysis thus, *b* value is fixed for each zone 1.08 and *a* value is estimated for each zone. Point source models established with a notion to use existing earthquake energy distribution and hence earthquake catalog has been used to create this model. In Peninsular India, details of existing faults and their potential is hardly available for establishing a good fault model. Thus, ten prominent faults or fault zones have been chosen based on the associated seismicity and geology of the region which include Narmada Son lineament, Allahbund fault etc. A buffer zone of 0.2 delta has been used on either side of the fault line to create an envelope rather than using the fault line (Figure 6.13). The envelope represents the possible region for rupture around the fault. Attenuation relations are required to compute ground acceleration thus, attenuation relation recommended by Global Earthquake Model (GEM) committee has been considered for similar tectonic setting. Two models Atkin06 and Toro97 considered for Peninsular (Stable continental region). However, Gujarat has a different tectonic setting than rest of the Peninsular region, thus, considered as

active crustal region. For Gujarat, Akkar & Bommer 2010 model was considered from GEM recommendation.

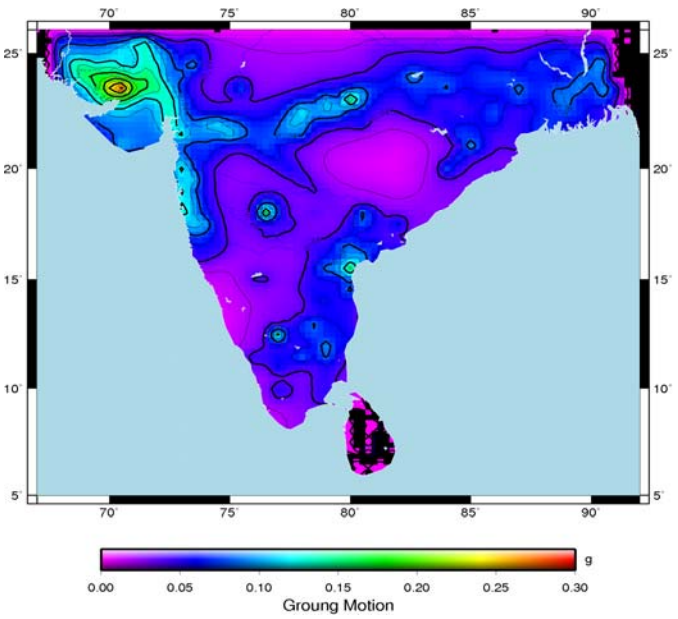

Figure 6.14 Probabilistic seismic hazard map of peninsular India showing spatial distribution of peak ground acceleration estimated for 10% probability of exceedance in 50 years, which correspond to return period of 475 years. PGA values are computed based on logic tree formulation.

The estimation of probabilistic seismic hazard for a region is represented by the annual exceedance rate of ground-motion parameter above a certain level. The Probabilistic seismic hazard map for PGA, at 10% probability of exceedance in 50 year with average return period of 475, based on combination of logic tree is shown in Figure 6. From the hazard map (figure 6.14), highest ground-motion, PGA at 10% of exceedance in 50 years, observed in Runn of Kuchchh, Gujarat in the range of 0.14 to 0.26 near Bhuj then, followed by Narmada-Son Lineament with the highest 0.19g near Jabalpur. For Mumbai and Koyana, a similar PGA estimated with 0.1g.

Ashish, Daniela Kuehn, Imtiyaz A Parvez and Conrad Lindholm**
*NORSAR, Norway

6.14 Neo-Deterministic Seismic Hazard Map of India

Rapid urbanization, development of critical structures and lifelines, such as dams and Nuclear Power Plants, industrialization of cities and the concentration of populations, living or settling in hazardous areas, are all matters of growing concern. Thus, the recent social and economic development exposed to earthquake hazards implies future heavier loss of life and economic damage, unless reliable preventive actions are enforced following the rapid rise of interest about environment concerns and increased official and public awareness about earthquake hazard in India. The first ever neo-deterministic seismic hazard map of India by computing synthetic seismograms with input data set consists of structural models, seismogenic zones, focal mechanisms and earthquake catalogues was published 2003 by C-MMACS. Last decade has witnessed an increased activity in seismological experiments and provide more detailed and denser information of subsurface structures. Now, there is a need to revise the existing deterministic hazard map with high-resolution structural model, new available focal mechanism data, extended source types and updated earthquake catalogues. The present study is aimed to generate and new updated NDSHA map for India with updated inputs available till date. Realistic synthetic seismograms are constructed by the modal summation technique to model ground motion at the sites of interest, using the available knowledge of the physical process of

earthquake generation (source position and orientation of the focal mechanism), level of seismicity (distribution of maximum observed magnitude) and wave propagation in anelastic media. From these synthetic signals engineering parameters can be extracted in order to assess the seismic hazard. Therefore, we can also estimate these parameters in those areas where very limited (or no) historical or instrumental information is available. As examples of the results that can be obtained, we show the maps of the distribution of maximum displacement (D_{max}), maximum velocity (V_{max}) and design ground acceleration (DGA) over the investigated area.

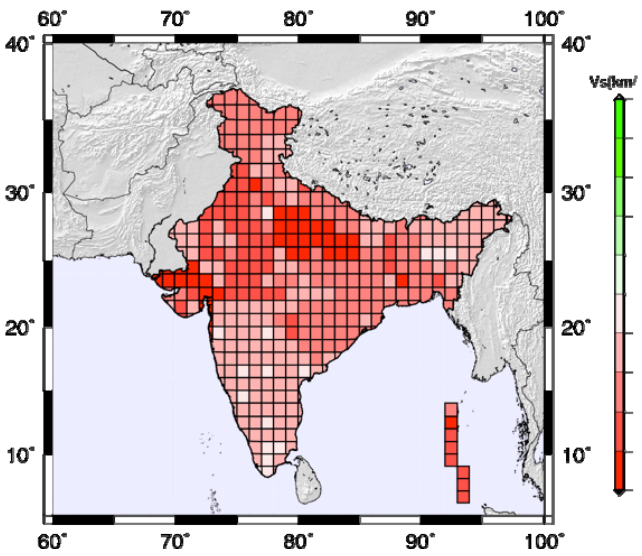

Figure 6.15 Shear wave velocity Vs in the upper most layer for each 1x1 degree cell.

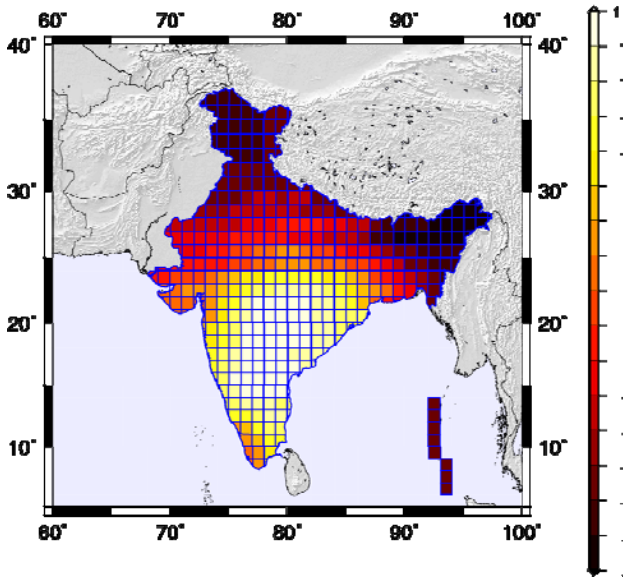

Figure 6.16 The distribution of Qs at each 1 x degree cell in the uppermost layer.

In order to revise the deterministic seismic hazard map, firstly a high-resolution velocity map at 1 x 1 degree cells of resolution have been prepared constituting 387 cells, which include subcontinent region Nepal, Bangladesh, Bhutan and Andaman & Nicobar Island. For each cell, the structural parameters that contain P wave velocity, S wave velocity, density, layer thickness, Qp and Qs are compiled. An example of shear wave velocity Vs and Qs of upper most layers is shown in figures 6.15 and 6.16 respectively. Earthquake catalogues and databases are other important parameters and in the present study, the earthquake data set spanning the time interval from 25 to 2011 has been used based on pre-instrumental and historical macro seismic information. We have used the database from the international agencies like NOAA, ISC, NEIC, CNSS, CMT and national agencies like IMD and NDMA and several published research papers. Figure 6.17 shows the smoothed seismicity map of India and adjacent areas along with the representative focal mechanisms in figure 6.18. The simulated seismograms are efficiently computed with the modal summation technique for 1 Hz considering layered anelastic models for wave propagation, which are representative of the average properties of the crust and upper mantle along the considered source site paths. However, we could also extend the computations to higher frequencies (5 or 10 Hz), and are planning to implement the use of a finite source model for the scaling. From the set of complete simulated seismograms, various

engineering parameters e.g. the Maximum displacement, velocity, acceleration and Designed Ground Acceleration (DGA) have been extracted.

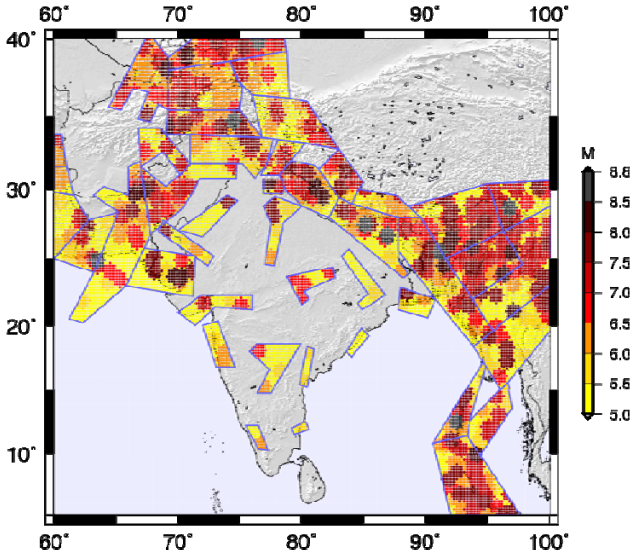

Figure 6.17 The smoothed seismic sources plotted in the respective seismogenic source zones used for the computation of synthetic seismograms

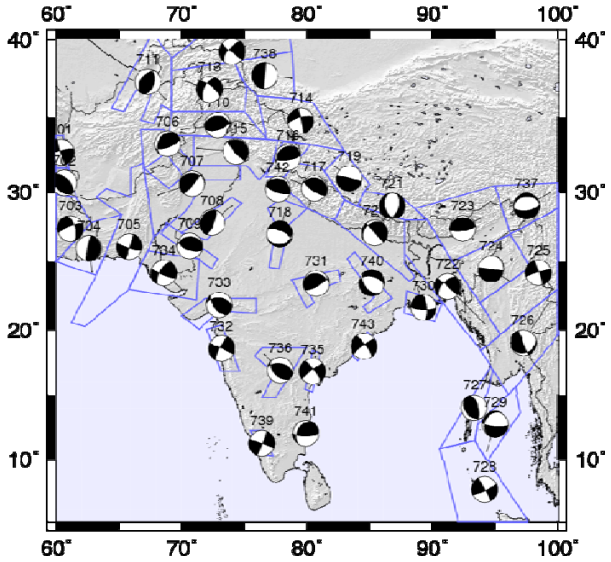

Figure 6.18 Seismogenic Zones defined on the basis of geology, tectonics, earthquake catalogue and the earthquake focal mechanism for each zone.

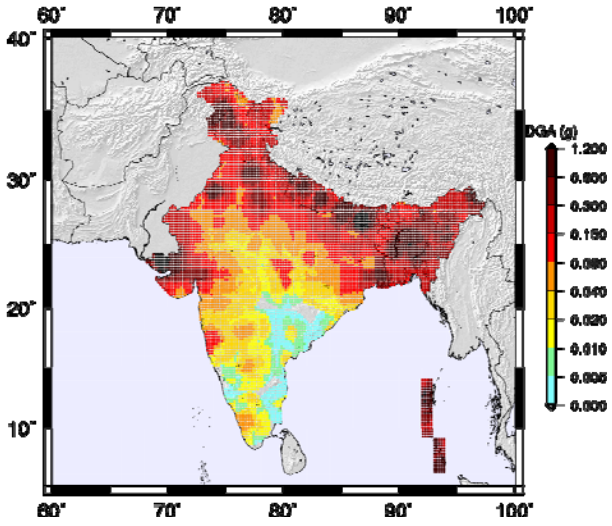

Figure 6.19 Spatial distribution of the estimated design ground acceleration in g.

The maximum values of DGA have been estimated over the northeast Indian region in the epicentral zone of the great Assam earthquakes of 1897 and 1950 (Figure 6.19). The DGA values obtained for this region fall in the range above 0.6 g. The Bihar-Nepal and Central Himalayan region have DGA values between 0.3 and 0.6 g. In part of western Uttar Pradesh and in the epicentral zone of the Uttarkashi earthquake of 1991 the estimated DGA values are between 0.15 and 0.3 g.

Imtiyaz A Parvez, Andrea Magrin, Franco Vaccari*, Ashish, Ramees R Mir and Panza G F**
*Department of Mathematical and Geosciences, University of Trieste, Italy

6.15 Crustal Imaging of Dharwar Region across E-W Corridor

Some of the fundamental problems confronting Earth scientists are to understand the structure, dynamics, origin and evolution of continental crust. An experiment was designed to study the crustal and mantle structure along the east-west corridor across Dharwar Craton for constraining models of crustal evolution. CSIR-4PI (erstwhile C-MMACS) has collaborated with

the National Geophysical Research Institute (NGRI), Hyderabad and operated broadband seismometers in locations throughout India with research interests centered on the southern Indian shield. During the period between April 2010 and March 2013 twelve stations were operated on an approximately straight SWW-NEE line in East and West Dharwar Craton and distributed along approximately straight line with an average spacing of 15 km with a greater density in the middle of the profile as low as 5 km.

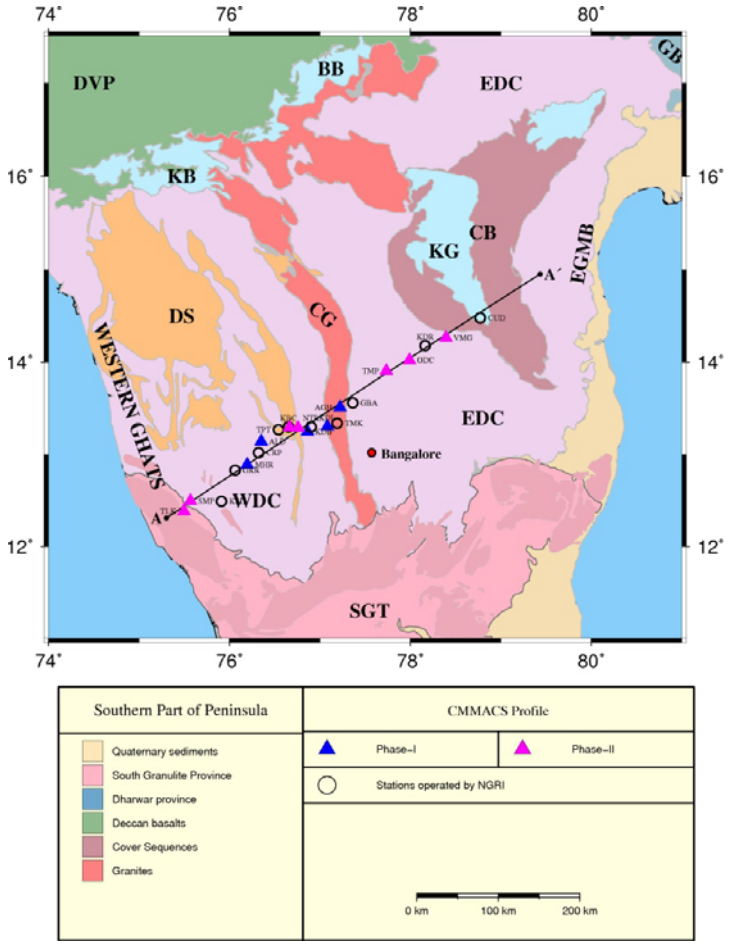

Figure 6.20 Major Geological terrains, tectonic features of Dharwar Craton and seismic stations (pink and blue triangle and black circle) operated in the region. Profile AA' represents the section along which stations are projected. EDC: East Dharwar Craton; WDC: West Dharwar Craton; SGT: Southern Granulite Terrain; DVP: Deccan Volcanic Province; CB: Cuddapah Basin; KB: Kaladgi Basin; BB: Bhima Basin.

Earthquake waveform data (recorded at 100 sps) is archived regularly. Teleseismic earthquake waveforms were extracted based on USGS earthquake catalog from data archive and converted to SAC format. The receiver function is calculated by using time domain iterative deconvolution for all distant earthquakes representing the time delay between direct P and P to S converted phase from an interface and time delay corresponds to the depth of the interface (see figure 6.20). The amplitude vector for each receiver function (corrected for the effect of incidence angle) is back-projected along a ray-path calculated for a standard earth model. In this case, IASP91 global model was used to convert travel times from the P-S conversion into depth. The volume along the profile was divided into bins of 1 km height and length along the profile but with a very wide dimension perpendicular to the profile. Amplitudes of the rays traversing each bin were summed and averaged to give the amplitude of the bin.

The strike of the Dharwar in this region is roughly north south and to allow for the oblique angle of profile AA' (figure 12), stations have been projected on to the profile along lines AA'. Ideally, the location of stations should fall precisely along the profile but in practice they are scattered by up to 20 km to either side. The resulting CCP depth migration for profile AA' is plotted in Figure 13. The crust-mantle boundary is clearly visible beneath the Dharwar craton as the only laterally continuous strong amplitude positive interface. In east Dharwar, The general trend is flat Moho

at a depth of 36-38 km. On the other hand in west Dharwar, Moho depth varies from 42-44 km and a presence of strong intra-crustal amplitude at a depth of ~15 km.

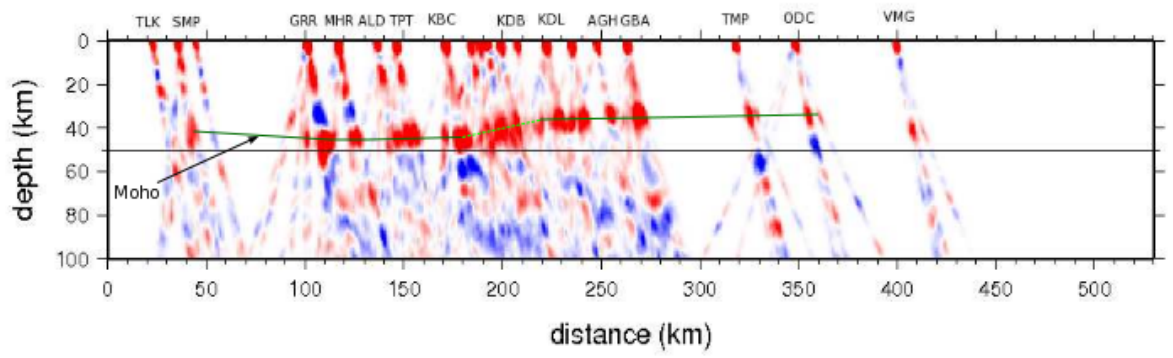

Figure 6.21 CCP depth-migrated receiver function profile along Profile AA'. The interpreted Moho is marked as a small green solid line and a dotted line for possible transition zone of contact between East and West Dharwar craton.

Transition zone between east and west Dharwar Craton observed between chitradurga schist belt and closepet granite represented/sampled by stations NTR, KDB, GRH, BRS and KBC (see Figure 6.21). This zone shows a smooth variation in moho depth

Ashish and Imtiyaz A Parvez

6.16 Seismic Broadband Experiment in Kashmir Himalayas

Five broadband seismic stations in Kashmir Valley are operational in continuous mode from June 2013 and recording seismic data at 100 samples per second using ~80 W solar panels for uninterrupted power supply. The second phase of this project will be operational this year with 10 more stations to get a clearer picture of crust and upper mantle of the Kashmir valley, which will eventually enhance our understanding of rheology of this region (figure 6.22).

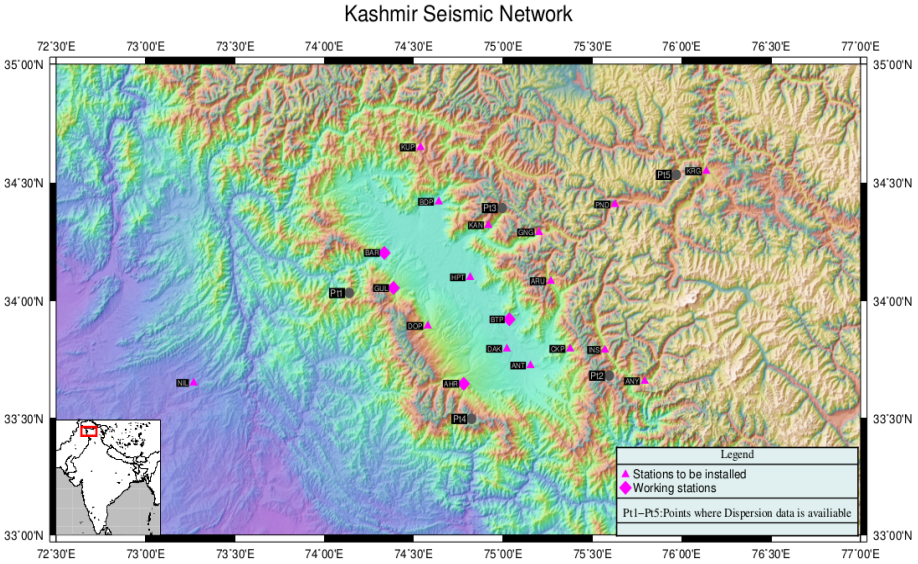

Figure 6.22 Proposed and currently working seismic stations. Diamonds are the currently working stations (from June 4, 2013), triangles are the proposed stations some of these sites were visited last year. NIL is Nilore Pakistan IRIS station whose data is freely available online.

Using four stations (Aharbal, Batpal, Gulmarg and Baramulla) data, we have estimated crustal structure beneath these seismic broadband stations in Kashmir valley from receiver function analysis. Seventy earthquakes (figure 6.23) with good signal to noise ratio, magnitude >= 5 and epicentral distance between 30 and 90 degrees were chosen to determine the S wave velocity structure beneath each station. Three of the stations were located on Pir Panjal range of Kashmir Himalaya. We use receiver function data, which are sensitive to velocity transitions and vertical travel times, together with surface-wave dispersion measurements, which are sensitive to the average velocity but relatively insensitive to sharp velocity contrast, to estimate the variations of crustal structure beneath four stations in Kashmir Himalaya. To avoid bias in the inversion, we have used the same AK135 continental model whose lower part is not permitted to change at all stations. Receiver function data was prepared before the joint inversion by setting the time from -45 to +57 seconds and header of each was filled with value of Gaussian width value (1.6), ray parameter. Receiver functions with close value of delta and backazimuth were binned together to increase the signal to noise ratio. At all stations starting model was Kennet's AK135. Inversion sensitivity has been tested by varying parameters, like influence parameter 'p', damping factor and fixing Vp/Vs or Vp only. For tests done on various value of damping factor and p value, we chose the value of p ~ 0.1 for all stations, the results for AHR station are given in figure 6. It is evident from inversion results that region is quite complex in crust and upper mantle.

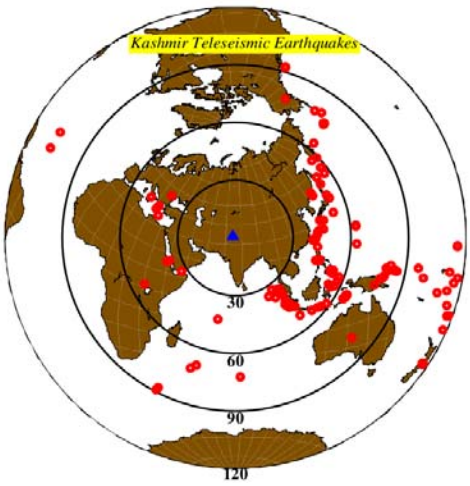

Figure 6.23 Teleseismic earthquakes (red circles) recorded by four seismic stations (Blue triangle) in Kashmir valley. The events having epicentral distance in the range 30 to 90 degrees were used for receiver function study.

The radial receiver function have first Moho multilple received at about 6.5 sec, H-k stacking revealed a complex behavior of the crustal which can be due to different mid-crustal layers. Receiver functions were jointly inverted with fundamental mode Rayleigh wave velocity to constraint the crustal thickness beneath each station. The results satisfy the predictions of H-k stacking as all the four stations reveal complex seismic crustal structure.

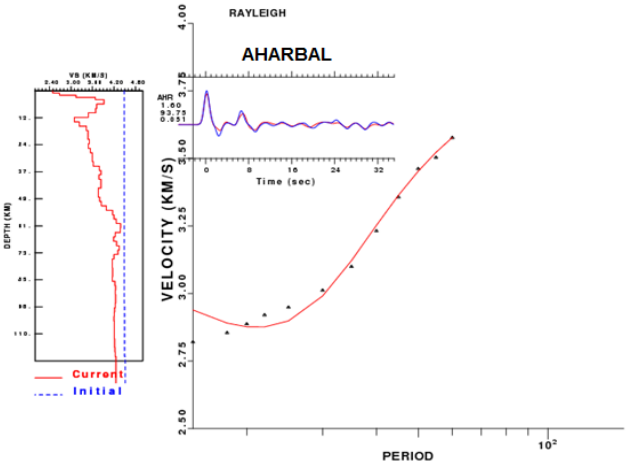

Figure 6.24 Joint inversion results for Aharbal seismic station.

Moho beneath each station varies in the range of 50-55 km. Moho at BTP has to

slightly deeper than the other three stations as this station is more northwards and due to northward subduction of Indian plate beneath the Eurasian plate the Moho has to be slightly deeper here than of other two stations (AHR and GUL) which are located on Pir Panjal range of Kashmir Himalaya. Moho beneath Aharbal (AHR) station was found about ~52 Km , Gulmarg (GUL) ~55 Km, Baramulla (BAR)~ 52 Km and Batpal (BTP) ~ 56 Km. Vp/Vs ratio at all stations is in the range of 1.73 to 1.76.

Imtiyaz A Parvez, Ramees Mir and Ashish

6.17 Finite Element Method for Deformation in Porous Thermoelastic Material with Temperature Dependent Properties

The present study is focused on the numerical investigation in time domain of the deformation in thermoelastic material with one relaxation time (Lord and Shulman theory) with voids under dependence of modulus of elasticity and thermal conductivity on reference temperature. For numerical investigation of the concern problem, the finite element method with eight node isoparametric finite elements has been used. The results demonstrate that finite element method can reliably predict the deformation of the medium. Our results illustrate the temperature distribution, the displacement component, volume fraction field and the stresses.

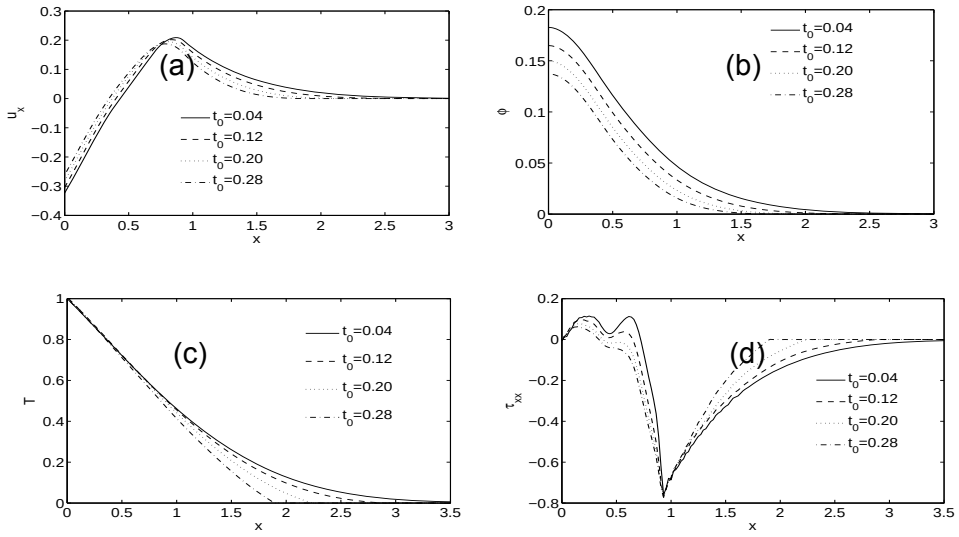

Figure 6.25 Horizontal displacement of solid particles (a), Volume fraction field (b), Temperature distribution (c), distribution of tangential stress component (d), with respect to *x* for different thermal relaxation time t_0 at *y=0*.

From figure 6.25, we observed that obtained results satisfy the prescribed boundary (stress free surface) conditions. We find that the relaxation time t_0 has a significant effect on the field variables (displacement, temperature, volume fraction field and stresses), as expected. As increase of distance *x* the effect of thermal shock on the field variables is reducing till a certain distance then after it is almost zero. The maximum temperature (T) and volume fraction field (Φ) has been found at the surface x=0.

Sushant Shekhar and Imtiyaz A Parvez

6.18 Finite Element Analysis of Wave Propagation in Thermoelastic Saturated Porous Medium

A general finite element approach is used for the numerical investigation of the wave propagation in transient thermoelastic saturated porous media in time domain. For that, the Biot's theory for wave propagation in saturated porous solid is modified to study the effect of thermal shock in the thermoelastic porous medium. Our results present the displacements of the fluid and solid particles, temperature distribution and the stresses over the surface and in depth. The effect of thermal shock on the surface of the half space $x \geq 0$ has been discussed and comparison has been made with the results predicted for the given field variables (displacements, temperature and stresses) for given depths (y = 0 and y = 1).

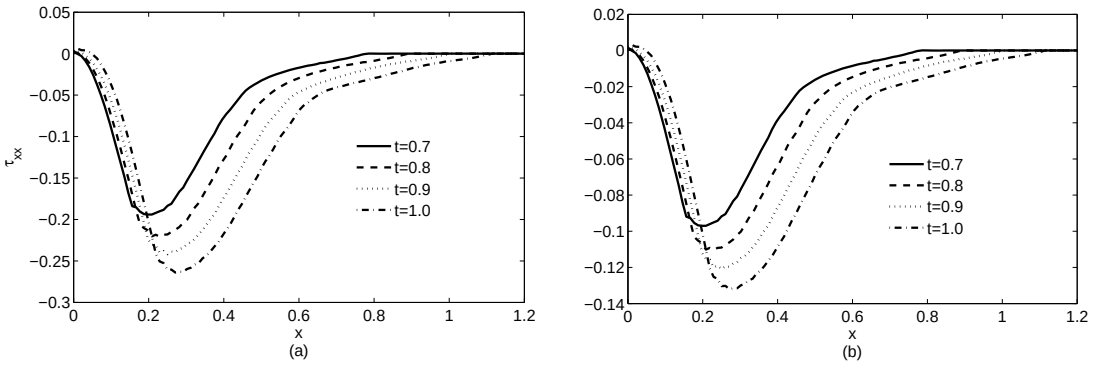

Figure 6.26 The distribution of tangential stress component with respect to x for different time step; (a) y=0, (b) y=1.

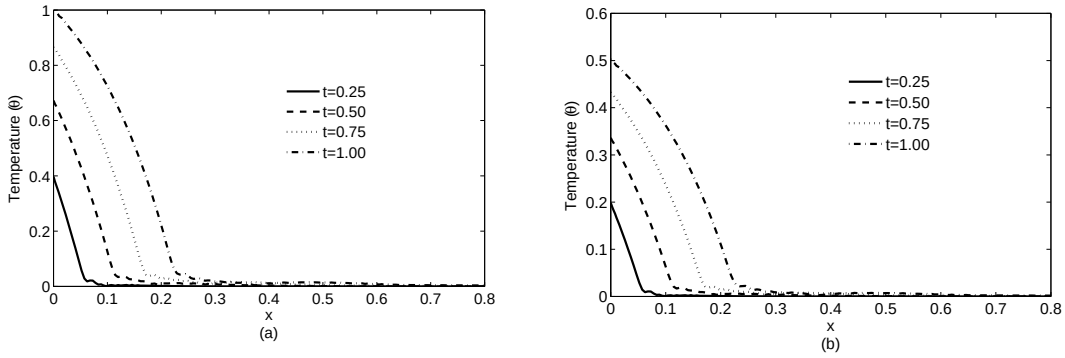

Figure 6.27 Temperature distribution with respect to x for different time step; (a) y=0, (b) y=1.

The numerical results satisfy the stress free boundary conditions that have been shown in figure 6.26. The thermal shock is applied on the surface x=0 therefore the maximum temperature will be at boundary zones, has been shown figure 6.27. From the numerical results, we observed that the study time has significant effect on the field variables, as expected. The thermal shock effect on the field variables is reducing from (y = 0 to y = 1) and its effect is clearly shown in figures 6.26 and 6.27 which satisfy the assumed boundary condition.

Sushant Shekhar and Imtiyaz A Parvez

6.19 Finite Element Method for Transient Wave Problem in Thermoelastic Saturated Poro-Viscoelastic Medium

The present study is aimed to the numerical investigation in time domain of the mechanical wave propagation through thermoelastic saturated poro-viscoelastic soil, involving complete Biot's theory. All the coupling and a hysteretic Rayleigh damping are taken into consideration for this study. For numerical investigation of the present problem, the finite element method with eight node isoparametric finite elements has been used. Our results illustrate the temperature distribution, the displacement components of solid and liquid phases and the stresses. An appreciable effect of damping coefficient η and relaxation times t_0 is observed on various results. We show the transient effect of thermal shock on the particle displacements, temperature and stresses in thermoelastic saturated porous medium.

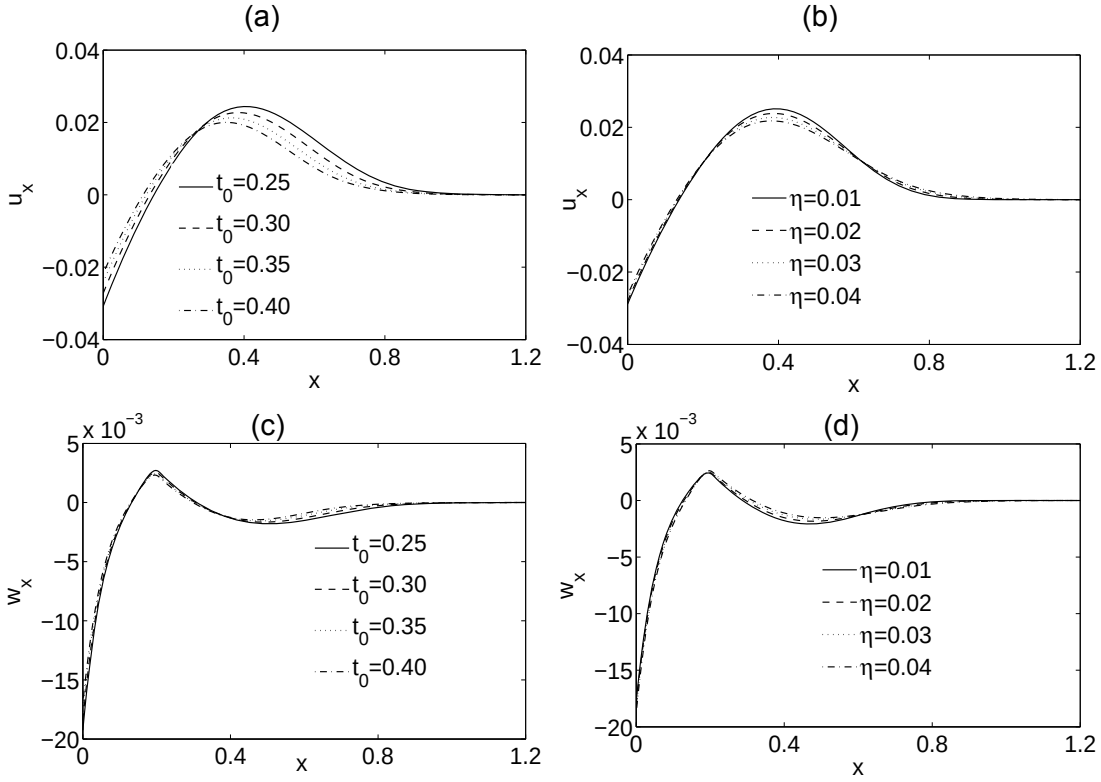

Figure 6.28 Horizontal displacements (u_x,,w_x) of solid and fluid particles with respect to x for different values of thermal relaxation time t_0 (a) and (c) and for different values of damping coefficient η (b) and (d)

We observe that the obtained results satisfy the prescribed boundary conditions. We find that the relaxation time t_0 and damping coefficient η have significant effect on the field variables (horizontal displacement of solid and fluid particles), as expected (figure 6.28). As increase of distance x the effect of thermal shock on the field variables is reducing and finally its value is zero.

Sushant Shekhar and Imtiyaz A Parvez

6.20 2004 M 9.3 Sumatra-Andaman Rupture Extent and Slip Distribution, and its Implications on the Regional Tectonics

2004 M 9.3 Sumatra-Andaman earthquake was one of the biggest instrumentally recorded plate-boundary event. For this study, we complied various published surface deformation values, which are observed using precise geodetic techniques, and reported by various agencies in and around the Sumatra-Andaman region to estimate a co-seismic slip distribution model. A fault geometry of along arc dip angle range between 8-12 degrees with a thrust to oblique thrust mechanism and depth of rupture extending not deeper than 30 km gave the best fit surface displacements for the near and far-to-the source sites for both the horizontal and vertical offset values. We specified the fault surfaces in 3 dimensions by nodes which are given by their longitude and latitude and depth. Nodes are placed along depth contours of the faults and each depth contour has the same number of nodes. The co-seismic slip amplitude was then estimated at these nodes. This elastic deformation was calculated by integrating over small patches in the regions between these nodes using the Okada method.

Based on the estimated slip distribution, there was a significant slip extending to the shallower portions near the trench axis over most of the southern part of the rupture (Sumatra and Nicobar Islands), but not in the Andaman segment. At the north and southern

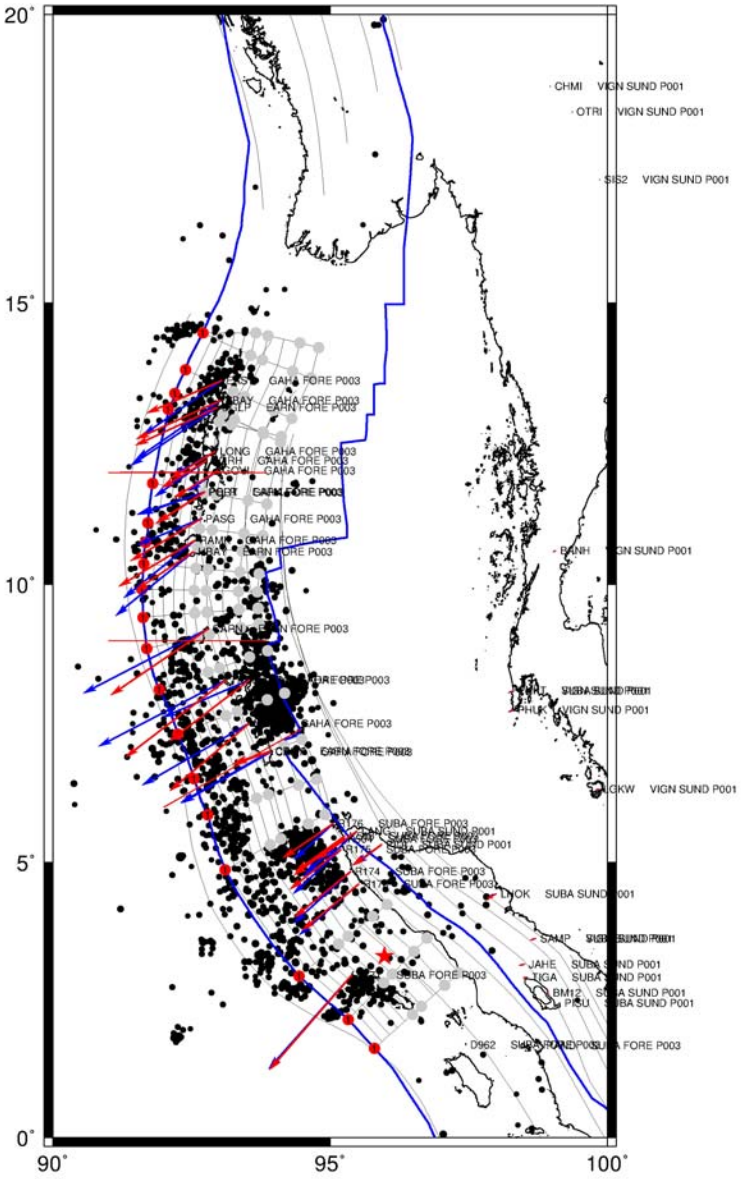

Figure 6.29 Co-seismic surface displacements observed (blue arrows) and predicted (red arrows) around the Sumatra-Andaman region for the 2004 M 9.3 earthquake (red star for location). Four character codes represent the GPS site followed by source publication and the code of tectonic plate it belongs. Filled circles are the fault nodes where red ones are considered to be on the ocean floor and grey ones are on the sub-surface on respective depth contour lines. Black filled circles are the aftershocks till 1st January, 2005. Blue lines are major tectonic boundaries.

ends of the rupture, the rupture was confined to the deeper portions of the plate interface, and these two segments have a steeper dip and greater depth than the rest. Slip magnitude varies considerably over the rupture, averaging ~16 m for the Sumatra and Nicobar region, and 5-8 m for most of the Andaman section. This model predicts a patch of very high slip offshore of Port Blair. Along arc rheological variations are not taken care in this model, which do have an effect on the slip distribution.

Anil Earnest

6.21 Establishment of Real-Time Data Telemetry VSAT's for Andaman GNSS Network

Geodetic monitoring does have significant scientific importance in understanding the deformational rates, fault-slips and kinematics of a plate boundary zone. High-rate geodetic observations help in identification of zones with sudden variations in slip-rates or zones with silent or slow slips. CSIR-4PI (erstwhile C-MMACS) has initiated a network of high rate GNSS observatories along the Andaman & Nicobar Island chain to understand the nature of tectonic processes happening along this margin for the past few years called Andaman Nicobar Geodetic Network (ANGN). Real-time analysis of the hence collected data from these observational networks can shed new insights on the seismogenic processes there but needs a data relay setup from Andamans to the data receipt/analysis setup at CSIR-4PI (erstwhile C-MMACS). Earlier we had setup a real-time GNSS data receipt and analysis engine at CSIR-4PI (erstwhile C-MMACS) and has tested it using global real-time IGS data streams. As part of this initiative, we made a network of real-time data relay from the earlier established 3 CGPS sites at Andamans and a newly established CGPS site using VSAT terminals through ERNET, India. These sites are provided with 64kbps dedicated bandwidth to stream-out the data to CSIR-4PI (erstwhile C-MMACS) servers or to reach the Internet enabled receivers for maintenance.

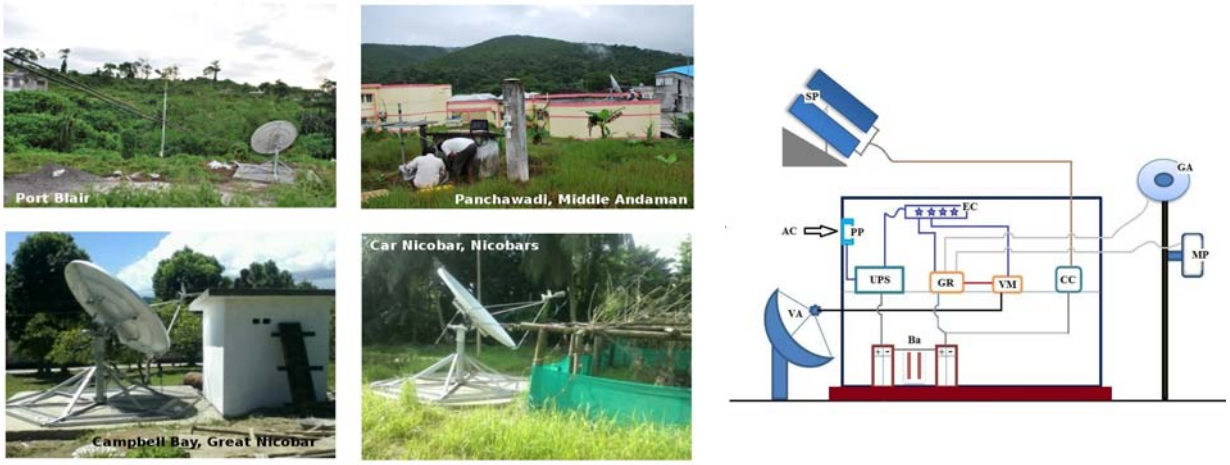

Figure 6.30 a) Data-relay VSAT setups established at Port Blair, Panchawadi, Campbell Bay and Car Nicobar (clockwise). b) Schematic diagram of the established setup at a GNSS site at A&N Islands. AC – External power supply, PP – Distribution Box, EC – Circuit Breaker, VA-- VSAT Antenna, CC— 10Amp Solar Charge Controller, Ba – SMF Battery, MP — MetPACK, GA — GNSS Antenna, VM—VSAT Modem, GR — GNSS Receiver, UPS -- UPS, SP — Solar PV module.

The newly established station is located at Campbell Bay, Great Nicobar the southern-most tip of Indian political territory, a zone of high amount of seismicity with it proximity to the Andaman trench and the West Andaman Fault. All the CGPS sites are collocated with met-packs. Real-time GNSS tracking data is being stored and analyzed at CSIR-4PI (erstwhile C-MMACS) servers located at Bangalore. A web-front-end is being developed for data/results dissemination for the ANGN. This research initiative is being implemented with the local logistical support of various government agencies of A&N Administration like Dept. of Agriculture, Dept. of Light House and Light Ships, Navodaya Vidyalaya, Pondicherry University and Dept. of Animal Husbandry and Veterinary Services.

Rajeev Krishnan, Sunilkumar T C, Anil Earnest and Vijayan M S M

6.22 Source Process of the Sikkim earthquake 18th September, 2011, Inferred from Tele-Seismic Body-Wave Inversion.

A moderate earthquake of magnitude Mw 6.9 occurred on 18 September 2011 at north Sikkim which is close to the Sikkim-Nepal border. The hypocenter parameters determined by the Indian Meteorological Department (IMD) shows that the epicentre is at 27.7°N, 88.2°E and focal depth of 58 km, located closed to the north-western terminus of Tista lineament. The epicentral region of Sikkim bordered by Nepal, Bhutan and Tibet, comprises a segment of relatively lower level seismicity in the 2500km stretch of the active Himalayan Belt. The largest historically known great earthquake in its vicinity is the 1934 Bihar Nepal border earthquake of M 8.3, located to the south-west of Sikkim, an event that caused intensity VIII damage in the Sikkim Himalaya. The north Sikkim earthquake was felt in most parts of Sikkim and eastern Nepal; it killed more than 100 people and caused damage to buildings, roads and communication infrastructure. Several landslides and rock falls followed the earthquake, which increased the death toll and impaired rescue operations. The National Earthquake Information Centre (NEIC) of US Geological Survey (USGS) located the epicentre of the main event to the immediate west of the IMD location. The focal mechanism solution for the main shock suggests dextral strike-slip faulting, possibly along a NW-SE oriented fault. This trend is consistent with the structural trend defined by the well located micro-earthquakes as well as the fault plane inferred from focal mechanisms.

We used the teleseismic body wave inversion methodology technique to determine the earthquake source parameters and the kinematic rupture process of the fault. This technique has been successfully applied to many earthquakes. The study of the rupture process is important to understand the source properties of an earthquake. Different methods are developed both in time domain and in frequency domain. Langston and Barker (1981, 1982), developed a generalized inverse technique based on the moment tensor formalism. Teleseismic body wave inversion methodology was proposed by Kikuchi and Kanamori (1982, 1986 and 1991). In the first paper, a numerical method is developed to study complex body waves into a multiple shock sequences. Assuming that the events have identical fault geometry and depth, the far field source time function is obtained as a superposition of ramp functions. In the next

paper they considered a general case where the rupture process consists of sub events with arbitrary source parameters. And in the third paper they developed a method to determine the mechanism and the rupture process considering that the main fault consists of a set of sub faults, each of which could have different focal mechanism.

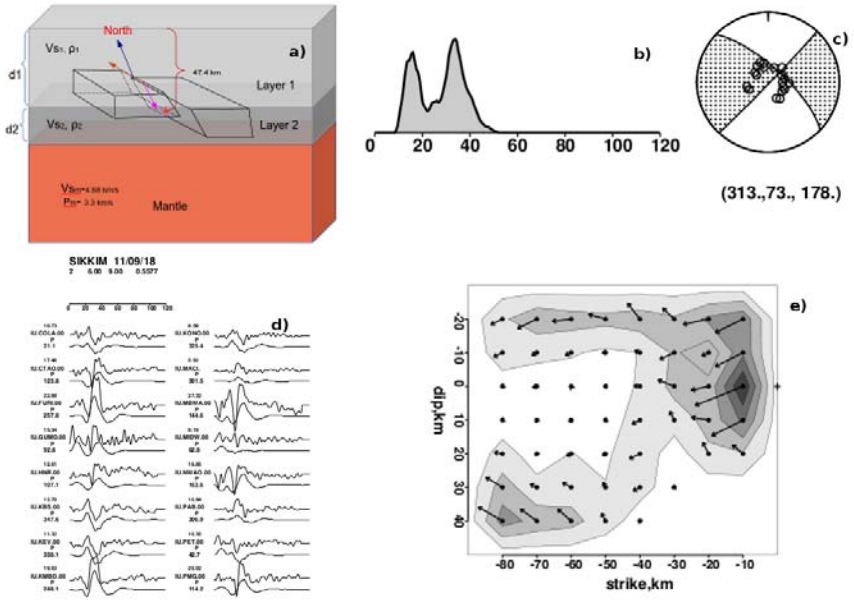

Figure 6.31 a) Schematic diagram of fault geometry used. b) Source time function used. c) Focal mechanism determined d) Comparison of the observed teleseismic body waveform data (upper trace) with the calculated waveform (lower trace). The numbers below the station code indicate maximum amplitude. and e) Distribution of co-seismic slip pattern along the strike.

The CMT and USGS focal mechanisms of the Sikkim event indicate strike-slip faulting. To determine the source parameters of this earthquake, body wave inversion modelling is applied using the methodology adopted by Kikuchi and Kanamori (1991). Broadband digital data were selected, recorded at teleseismic distances between 30-90 degrees with a good signal to noise ratio. Teleseismic distances in this range were used, in order to avoid upper mantle and core triplications and to limit the path length within the crust. Synthetic waveforms were generated using a simple triangular source time function, in order to determine the components of the moment tensor and the focal depth of the mainshock. The result of the inversion was a focal mechanism indicating strike slip type faulting at a depth of 44.7 km. The total seismic moment M_o = 2.42 x10^{26}dyn·cm equivalent to Mw = 6.9 earthquake was obtained through this study. This is consistent with the Global CMT and USGS solution. The determined fault plane solution is: strike, φ=313°, dip, δ=73° and rake, λ =163°. From this model, we found out that the average slip value of Sikkim earthquake is 0.3979m.

Sunilkumar T C and Anil Earnest